Proceedings of the 2004 IEEE
International Conference on Control Applications
Taipei, Taiwan, September 2-4, 2004

High Performance Position Controller for PMSM Drives Based on TMS320F2812 DSP

Ying-Shieh Kung, *Member, IEEE* and Pin-Ging Huang

***Abstract*—This paper presents a high performance position controller for drives of permanent magnet synchronous motor (PMSM) using a TMS320F2812 DSP chip. Due to the new generation DSP (Digital Signal Processor) has the characteristics of the fast computation (150MIPS) and the complete peripheral circuits for motor drive, therefore a fully digital controller of PMSM drives system, which includes current vector control scheme, SVPWM generation, A/D conversion, coordinate transformation, QEP detection and an intelligent strategy, can be integrated and realized by software within a DSP chip. For increasing the performances of PMSM drives, an adaptive fuzzy controller constructed by fuzzy basis function and a parameter adjustable mechanism is proposed and applied in position control loop to cope with the system uncertainty and to increase a fast tracking response. To confirm the effectiveness of the proposed system, an experimental system included by a PMSM, DSP control board, inverters, rectifier have been set up and some experimental results have been validated the theoretical ones.**

I. INTRODUCTION

Owing to the advantages of the superior power density, high performance in motion control - fast positioning and better accuracy, permanent magnet synchronous motors (PMSM) have gradually used in many automation control fields as an actuators [1], such as computer-controlled machining tools, robotic systems and semiconductor manufacturing equipments. But in industrial applications, there are many uncertainties, such as system parameter uncertainty, external load disturbance, friction force, unmodeled uncertainty, always diminish the performance quality of the pre-design of the motor driving system. To cope with this problem, in recent years, many intelligent control techniques [2-4], such as fuzzy control, neural networks control, adaptive fuzzy control, etc., have been developed and applied to the precision position control of servo motor drives to obtain high operating performance. A high performance motor control system should have a fast dynamic response in adjusting its control parameters so that the motor outputs affected by the disturbances can recover to their original status as soon as possible [5].

Y.S. Kung is with the Department of Electrical Engineering, Southern Taiwan University of Technology, 710, Tainan, Taiwan (corresponding author, phone: 886-6-2533131 ext 3300; e-mail: kung@mail.stut.edu.tw).

P.G. Huang is with the Department of Electrical Engineering, Southern Taiwan University of Technology. (e-mail: tom01@ms41.url.com.tw).

With the rapid development in microprocessor, the high performance DSP chip becomes a popular research on digital control [6-7] for ac drives due to their high-speed performance, simple circuitry, on-chip peripherals of a micro-controller into a single chip solution. Especially the new generation DSP controller TMS320F28x [8] produced by Texas Instrument, which has the advantages of high speed (150MIPS) performance, up to 128Kx16 flash, 2 set (12 outputs) of PWM (Pulse Width Modulation) output, 2 set (4 inputs) of QEP (Quadrature Encoder Pulse) input, 12 channels 12-bit A/D converter (200ns conversion time), 56 bits GPIO, is very suitable to develop a fully digital controller and a complicated intelligent control algorithm in servo motor drives. Therefore, in this paper, a TMS320F2812 DSP embedded with the software of current vector control, SVPWM scheme and adaptive fuzzy control has been developed for a high performance position control for PMSM drives. With the excellent characteristics of the proposed system, it will make drives of PMSM more programmable, robust and easy implementation.

II. THEORETICAL ANALYSIS

The architecture of the proposed intelligent control system for a PMSM is shown in Fig. 1, where the current vector control and intelligent position control are all implemented within a TMS320F2812 DSP chip.

A. Current vector control

The configuration of the current loop for a PMSM is shown in Fig.1, and it includes PI controller, *Clarke*, modified $Clarke^{-1}$, *Park*, $Park^{-1}$ coordinate transformation, SVPWM, current detection pulse signal detection of the encoder, etc. After using vector control (control i_d^* to 0 in Fig.1), it will make the non-linear and coupling characteristics of PMSM become decouple. Thus, the torque magnitude control of PMSM is only need to control the current in the direction of q-axis. The transformations between stationary a-b-c frame, stationary α-β frame and synchronously rotating d-q frame [1] are shown in Fig.2, where $\bar{f}_s$ is a space vector refer to current, voltage or flux, and those transform equations are described as the following equations:

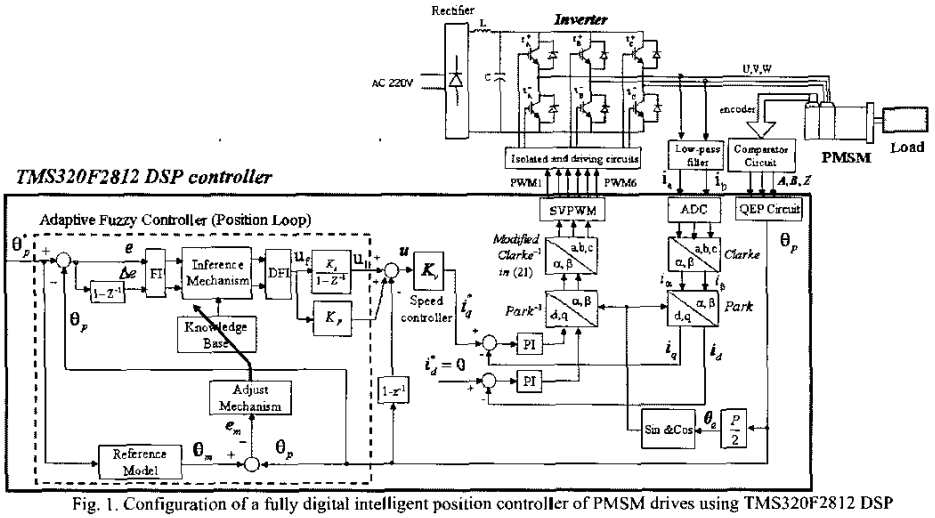

Fig. 1. Configuration of a fully digital intelligent position controller of PMSM drives using TMS320F2812 DSP

❑ *Clarke*: stationary a-b-c frame to stationary α-β frame.

$$\begin{bmatrix} f_\alpha \\ f_\beta \end{bmatrix} = \begin{bmatrix} \frac{2}{3} & \frac{-1}{3} & \frac{-1}{3} \\ 0 & \frac{1}{\sqrt{3}} & \frac{-1}{\sqrt{3}} \end{bmatrix} \begin{bmatrix} f_a \\ f_b \\ f_c \end{bmatrix} \quad (1)$$

❑ *Clarke*$^{-1}$: stationary α-β frame to stationary a-b-c frame.

$$\begin{bmatrix} f_a \\ f_b \\ f_c \end{bmatrix} = \begin{bmatrix} 1 & 0 \\ \frac{-1}{2} & \frac{\sqrt{3}}{2} \\ \frac{-1}{2} & \frac{-\sqrt{3}}{2} \end{bmatrix} \begin{bmatrix} f_\alpha \\ f_\beta \end{bmatrix} \quad (2)$$

❑ *Park* : stationary α-β frame to rotating d-q frame.

$$\begin{bmatrix} f_d \\ f_q \end{bmatrix} = \begin{bmatrix} \cos\theta_e & \sin\theta_e \\ -\sin\theta_e & \cos\theta_e \end{bmatrix} \begin{bmatrix} f_\alpha \\ f_\beta \end{bmatrix} \quad (3)$$

❑ *Park*$^{-1}$: rotating d-q frame to stationary α-β frame.

$$\begin{bmatrix} f_\alpha \\ f_\beta \end{bmatrix} = \begin{bmatrix} \cos\theta_e & -\sin\theta_e \\ \sin\theta_e & \cos\theta_e \end{bmatrix} \begin{bmatrix} f_d \\ f_q \end{bmatrix} \quad (4)$$

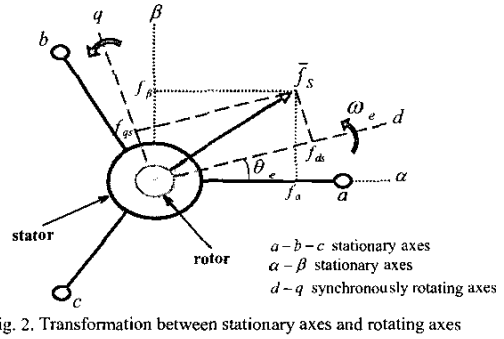

Fig. 2. Transformation between stationary axes and rotating axes

In Fig.1, the PMSM will be decoupled if control $i_d^* = 0$, thus we can control a PMSM as easy as to control a DC motor. Considering the load term, the electrical and mechanical equations of PMSM can be written as the follows:

$$T_e = K_i i_q^* \quad (5)$$

$$J_m \frac{d}{dt}\omega_p + B_m\omega_p = T_e - T_L \quad (6)$$

where T_e, K_i, J_m, B_m and T_L are motor toque, torque constant, inertial, damping ratio and load toque, respectively.

B. Space Vector Pulse Width Modulation (SVPWM)

SVPWM is a special switching scheme of a 3-phase power converter with the six power transistors. The typical structure of 3-phase power converter is shown in Fig. 3. According to the ON/OFF switching of upper transistors in Fig. 3, there have eight possible combinations. The eight vectors are called basic space vectors and they are denoted by U_0, U_{60}, U_{120}, U_{180}, U_{240}, U_{300}, O_{000} and O_{111}, which are shown in Fig. 4. Using the *Clarke* transformation, the project values in α-β axis for six basic space vectors can be obtained and are also shown in Fig. 4. The SVPWM technique is applied to approximate the reference voltage U_{out}, and it combines of the switching pattern with the basic space vectors. Therefore, the motor-voltage vector U_{out} will be located at one of the six sectors (S3, S1, S5, S4, S6, S2) at any given time. Thus, for any PWM period, it can be approximated by the vector sum of two vector components lying on the two adjacent basic vectors, as the following:

$$U_{out} = \frac{T_1}{T}U_X + \frac{T_2}{T}U_{X+60} + \frac{T_0(O_{000}\ or\ O_{111})}{T}, \quad (7)$$

where $T_0 = T - T_1 - T_2$ and T is half of PWM carrier period.

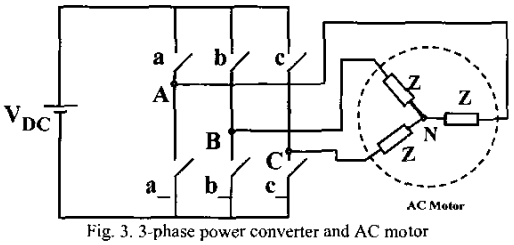

Fig. 3. 3-phase power converter and AC motor

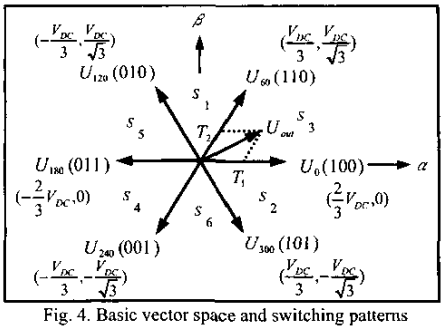

Fig. 4. Basic vector space and switching patterns

1) Calculation of T_1 and T_2: Any output voltage can be projected into each adjacent basic vector in SVPWM strategy. For example, the output voltage vector U_{out} in the sector S_3 can be the combination of U_0 and U_{60} shown in Fig.4. Therefore, the calculation of T_1 and T_2 can be shown as,

$$U_0 = \frac{2}{3}V_{DC}\vec{\alpha} \tag{8}$$

$$U_{60} = \frac{1}{3}V_{DC}\vec{\alpha} + \frac{1}{\sqrt{3}}V_{DC}\vec{\beta} \tag{9}$$

If we substitute (8)~(9) into (7), we obtain

$$U_{out} = \frac{T_1}{T}U_0 + \frac{T_2}{T}U_{60} = \frac{T_1}{T}(\frac{2}{3}V_{DC}\vec{\alpha}) + \frac{T_2}{T}(\frac{V_{DC}}{3}\vec{\alpha} + \frac{V_{DC}}{\sqrt{3}}\vec{\beta}) \tag{10}$$

$$\triangleq V_\alpha\vec{\alpha} + V_\beta\vec{\beta}$$

and compare the coefficient in (10), thus

$$T_1 = \frac{T}{2V_{DC}}(3V_\alpha - \sqrt{3}V_\beta) \tag{11}$$

$$T_2 = \sqrt{3}\frac{T}{V_{DC}}V_\beta \tag{12}$$

In the similar way, the T_1 and T_2 in other sector can be derived and be rearranged in TABLE I, which T_X, T_Y and T_Z are represented as the followings:

$$T_X = \sqrt{3}\frac{T}{V_{DC}}V_\beta \tag{13}$$

$$T_Y = \frac{T}{2V_{DC}}(3V_\alpha + \sqrt{3}V_\beta) \tag{14}$$

$$T_Z = \frac{T}{2V_{DC}}(-3V_\alpha + \sqrt{3}V_\beta) \tag{15}$$

If it is at the saturation condition $T_1 + T_2 > T$, the T_1 and T_2 should be modified as:

$$T_{1SAT} = T_1\frac{T}{T_1 + T_2} \tag{16}$$

$$T_{2SAT} = T_2\frac{T}{T_1 + T_2} \tag{17}$$

2) Determination of the duty cycles and CMPRx: After the calculation of T_1 and T_2, it has to re-transfer it to the duty cycles and CMPx values in DSP controller to generate the PWM output signals for controlling the power transistor switching time in Fig. 3. First, the duty cycles are defined as Ta_{on}, Tb_{on}, Tc_{on}, and calculated as the followings:

$$Ta_{on} = (T\text{-}T_1\text{-}T_2)/2 = T_0/2 \tag{18}$$

$$Tb_{on} = Ta_{on} + T_1 \tag{19}$$

$$Tc_{on} = Tb_{on} + T_2 \tag{20}$$

Then, the CMPR1~CMPR3 values can be obtained in TABLE II depend on the sector number. For example in S3 sector, its output waveforms PWM1~PWM3 are depicted in Fig. 5 with the duty time at U_0 (100), U_{60} (110) and zero vector (O_0 and O_{111}) be T_1, T_2, T_0, respectively.

3) Determination of the sector: To determine the sector, we first modified the $Clarke^{-1}$ transformation as follows,

$$\begin{bmatrix} V_{rfx} \\ V_{rfy} \\ V_{rfz} \end{bmatrix} = \begin{bmatrix} 1 & 0 \\ \frac{-1}{2} & \frac{\sqrt{3}}{2} \\ \frac{-1}{2} & \frac{-\sqrt{3}}{2} \end{bmatrix} \begin{bmatrix} V_\beta \\ V_\alpha \end{bmatrix} \tag{21}$$

then, the output waveforms of V_{rfx}, V_{rfy} and V_{rfz} for sinusoid wave inputs (V_α,V_β) can be calculated. They can determine the sector according to the following rules:

If $V_{rfx} > 0$ then a=1 else a=0
If $V_{rfy} > 0$ then b=1 else b=0
If $V_{rfz} > 0$ then c=1 else c=0
Sector = a+2b+4c. (22)

From equations (13)~(15) and (21), we have.

$$\begin{bmatrix} T_x \\ T_y \\ T_Z \end{bmatrix} = \frac{\sqrt{3}T}{V_{DC}} \begin{bmatrix} V_{rfx} \\ -V_{rfz} \\ -V_{rfy} \end{bmatrix}. \tag{23}$$

T_x, T_y and T_z can be derived directly from V_{rfx}, V_{rfy} and V_{rfz}.

TABLE I. T_1 AND T_2 IN ALL SPECIFIC SECTORS

	S_3	S_1	S_5	S_4	S_6	S_2
T_1	$-T_Z$	T_Z	T_X	$-T_X$	$-T_Y$	T_Y
T_2	T_X	T_Y	$-T_Y$	T_Z	$-T_Z$	$-T_X$

TABLE II. ASSIGNING DUTY CYCLE TO CMPx IN ANY SECTOR

Sector	S_3	S_1	S_5	S_4	S_6	S_2
CMPR1	Ta_{on}	Tb_{on}	Tc_{on}	Tc_{on}	Tb_{on}	Ta_{on}
CMPR2	Tb_{on}	Ta_{on}	Ta_{on}	Tb_{on}	Tc_{on}	Tc_{on}
CMPR3	Tc_{on}	Tc_{on}	Tb_{on}	Ta_{on}	Ta_{on}	Tb_{on}

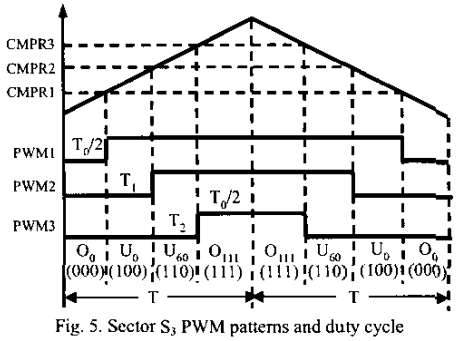

Fig. 5. Sector S_3 PWM patterns and duty cycle

4) Computation procedures of SVPWM design: SVPWM design is summary as following procedures.

Step 1: Determination of the sector according to the rule shown in (22), where V_{rfx}, V_{rfy}, V_{rfz} are the input signals of the SVPWM block circuit in Fig.1.

Step 2: Calculation of T_X, T_Y and T_Z from (23).

Step 3: Determination of T_1 and T_2 from Table 1. If it is at the saturation condition, we can use (16) and (17) to modify the T_1 and T_2.

Step 4: Determination of the duty cycle Ta_{on}, Tb_{on} Tc_{on} from (18)-(20).

Step 5: Assignment of the duty cycles to CMPR1, CMPR2 and CMPR3 from TABLE II.

C. Adaptive fuzzy controller in position control loop

The structure of an adaptive fuzzy controller for PMSM drives is depicted in the dotted line of Fig. 1, which consists of the fuzzy controller, a reference model and an adjusting mechanism. In Fig.1, the tracking error and the error change $e, \Delta e$ are defined as

$$e(k) = \theta_p^*(k) - \theta_p(k), \tag{24}$$

$$\Delta e(k) = e(k) - e(k-1), \tag{25}$$

and K_e*e, K_{de}*Δe and $u_f$as input and output variable of fuzzy controller, respectively. The design procedure of the fuzzy controller is as follows:

- Define the linguist value are $\{A_1, A_2, E\}$ with the symmetrical triangular membership function:

$$\xi_m(x_i, \bar{x}_i^m, w_i^m) = \begin{cases} 0 & x_i \le \bar{x}_i^m - w_i^m/2 \\ \dfrac{x_i - \bar{x}_i^m + w_i^m/2}{w_i^m/2} & \bar{x}_i^m - \dfrac{w_i^m}{2} < x_i < \bar{x}_i^m \\ \dfrac{\bar{x}_i^m + w_i^m/2 - x_i}{w_i^m/2} & \text{when } \bar{x}_i^m < x_i < \bar{x}_i^m + \dfrac{w_i^m}{2} \\ 0 & x_i \ge \bar{x}_i^m + \dfrac{w_i^m}{2} \end{cases} \tag{26}$$

  where x_i is input value, $\xi_m(\bullet)$ is output value, $\bar{x}_i^m$ and w_i^m are mean value and width of the triangular function.

- Derive M fuzzy control rules from the dynamic response characteristics [4] as initial condition, such as,

  IF e is A_1^m and Δe is A_2^m THEN u_f is E^m,m=1,2,..,M (27)

- Construct the fuzzy system with $u_f(\underline{x}|\underline{\theta})$ from those M rules using the singleton fuzzifier, product-inference rule, and central average defuzzifier method. Therefore, (27) is replaced with the following expression:

$$u_f(\underline{x}|\underline{\theta}) = \frac{\sum_{m=1}^{M} c_m[\prod_{i=1}^{2} \xi_m(x_i, \bar{x}_i^m, w_i^m)]}{\sum_{m=1}^{M}[\prod_{i=1}^{2} \xi_m(x_i, \bar{x}_i^m, w_i^m)]} \triangleq \frac{\sum_{m=1}^{M} c_m \mu_m}{\sum_{m=1}^{M} \mu_m} \tag{28}$$

  where those $c_1, c_2, .., c_M$ are adjustable parameters.

The gradient descent method is adopted to derive the adaptive control law in Fig. 1. The main purpose of adjusting the parameters of the fuzzy controller is to minimum the square errors (instantaneous cost function) between the rotor position and the output of the reference model. The instantaneous cost function is defined as follows:

$$J(k+1) = \frac{1}{2} e_m(k+1)^2 = \frac{1}{2}[\theta_m(k+1) - \theta_p(k+1)]^2 \tag{29}$$

and the parameters of c_j will be adjusted with,

$$\Delta c_j(k+1) \propto -\frac{\partial J(k+1)}{\partial c_j(k)} \tag{30}$$

To derive the formulation of adjusting the parameters c_j, at first, we assume T_L to be zero and take Laplace transformation with (5)-(6), and then

$$\frac{\theta_p(s)}{i_q^*(s)} = \left(\frac{K_t}{B_m}\right)\frac{B_m/J_m}{s(s + B_m/J_m)} \tag{31}$$

The bilinear transformation is applied and the difference equation of ac motor drive system can be derived as

$$\frac{\theta_p(k)}{i_q^*(k)} = \left(\frac{K_t}{B_m}\right)\frac{(1 - e^{-B_m T/J_m})z^{-1}}{(1 - e^{-B_m T/J_m} z^{-1})(1 - z^{-1})}, \tag{32}$$

where z^{-1} is a back-shift operator, and T is the sampling period. In Fig.1, the current command, i_q^*, and the output of fuzzy controller u_f can be obtained by the following expression

$$i_q^*(k) = K_v(u_f(k-1) + (K_i + K_p)u_f(k) - \theta_p(k) + \theta_p(k-1)) \tag{33}$$

From (32) and (33), we have

$$\begin{aligned} \theta_p(k) = {} & (A + 1 - BK_v)\theta_p(k-1) - (1 - BK_v)\theta_p(k-2) \\ & + BK_v u_f(k-2) + BK_v(K_i + K_p)u_f(k-1) \end{aligned} \tag{34}$$

with $A = \exp(-B_m T/J_m), B = K_t(1-A)/B_m$.

Furthermore, according to the chain rule, the partial differential equation of $J(k+1)$ in (30) can be rewritten as

$$\frac{\partial J(k+1)}{\partial c_j(k)} = -\alpha e_m(k+1)\frac{\partial \theta_p(k+1)}{\partial u_f(k)}\frac{\partial u_f(k)}{\partial c_j(k)} \tag{35}$$

where α is learning rate. From (28), (34), (35) and (30), the parameters c_j of fuzzy controller in (28) can be adjusted at each control sampling interval by the following expression.

$$\begin{aligned} \Delta c_j(k) &= \alpha BK_v(K_p + K_i)\frac{\mu_j}{\sum_m \mu_m} e_m(k) \\ &\approx \alpha sign(B)K_v(K_p + K_i)\frac{\mu_j}{\sum_m \mu_m} e_m(k) \end{aligned} \tag{36}$$

Because the motor parameter B is not easy to know, the $sign(B)$ is employed to calculate in (36) and it is always one due to B be positive. The sign(.) denoted the sign operator.

III. EXPERIMENTAL SYSTEM AND RESULTS

The overall experimental system is depicted in Fig. 1, and it includes a TMS320F2812 DSP controller, a voltage source IGBT inverter and a PMSM. The power of the PMSM, rating speed, maximum speed and maximum torque are 2200W, 2000rpm, 4000rpm and, 1.1Kg*m respectively. The resistance and inductance of the PMSM are 0.63Ω and 2.77mH. The torque magnitude of the brake is adjustable within 0.2~5N*m. An incremental optical encoder (2500 ppr) has been installed to PMSM as the rotor's position sensor. The inverter has six IGBT type power transistors. The

collector-emitter voltage of the IGBT is rating 600V, the gate-emitter voltage is rating ±20V, and the collector current in DC is rating 25A. Input signals of the inverter are PWM signals from DSP chip. In Fig.1, the current vector control scheme, SVPWM generation, A/D conversion, coordinate transformation, QEP detection and intelligent position control strategy are all realized with the software in this DSP chip. The PWM switching frequency of inverter is designed with 16k Hz, dead-band is 1μs, and the control sampling frequency of current and position loop are 8kHz and 2kHz, respectively. The flow chart of main program and the interrupt service routine for digital motor control algorithm are designed and shown in Fig. 7. Those programs are coded with C language, the computation time of DSP for executing current loop is 3.6μs and executing adaptive fuzzy control algorithm of position loop is 16 μs.

To verify the correctness of SVPWM circuit in Fig. 1, an experimental block diagram is constructed in Fig. 7, where the input signal is a constant voltage with phase variations from 0 to 360 degree. The input signal through the transformation of Park^{-1}, modified Clarke^{-1} and SVPWM computation, then the output waveforms PWM1~PWM6 are generated. Those PWM1~PWM6 are serially connected to a RC circuit with 10Ω resistor and 47μf capacitor, respectively. The load torque of brake is set to 2N*m. As a result, the waveforms of PWM1, PWM3 and PWM5 are measured and shown in Fig. 8. The output waveform and the phase difference for any two PWM waveforms is 120^0, thus they have proven the correctness of SVPWM design. Furthermore, to validate the effectiveness of the current vector control in Fig. 1, we set the input current command as $(i_d^*, i_q^*) = (0A, 3.5A)$, the currents of i_d, i_q and corresponding to current in *a-b-c* axes are measured and shown in Fig. 9. The results have shown the measured current tracks current command very well. Above results validate the success of vector control, and it will make the PMSM decouple.

In experiment, an adaptive fuzzy controller in Fig. 1 is applied in position control loop to test the dynamic performance of PMSM. The fuzzy controller in this paper adopts the singleton fuzzifier, triangular membership function, product-inference rule, central average defuzzifier method. The parameter adjusting mechanism is based on gradient descent method. The transfer function of the reference model is chosen by a standard second-order system with the natural frequency of 40 rad/s and the damping ratio of 1. The parameters of K_e, K_{de}, Ki, Kp and Kv in Fig. 1 are chosen as 1, 1, 0.0046, 0.4, 0.7, respectively. For testing the learning effect and choosing an adequate learning rate α of the proposed controller, a square wave position command with amplitude of 0.24 π and 0.64 π radian and the load with 0.2 N*m is applied and thus the tracking results between the output of reference model and the measured rotor position of PMSM under different learning rate of 0.05 and 0.15 are shown in Fig. 10. At initial, the rotor position of PMSM tracks the output of reference model with oscillation, meanwhile the parameters of fuzzy controller continuous tuning toward reducing the error between the output of the reference model and the rotor position at each sampling interval. After one square period command, the parameters of fuzzy controller are almost tuned to the adequate value and the dynamic response of the rotor position can match the output of the reference model very well. It has also presented that when α is chosen as 0.05 in Fig. 10(a), the learning is slow, but when α is 0.15 in Fig. 10(b), the position of the rotor can fast learns and tracks the output dynamic of the reference. Furthermore, to demonstrate the performance of the frequency response for the proposed controller architecture, the sinusoid tested signals for input commands are designed with amplitude of 0~1.6 π radians but different frequency with 1Hz and 3Hz, respectively. To reduce the phase-lag effect while sinusoid tracking, the bandwidth of the reference model in Fig.1 is chosen by 1/10 times than those in the experiment of the step response. Under this condition, the experimental results for the rotor position of PMSM tracks two tested signals are shown in Fig. 11(a) ~ Fig. 12(a), and the tracking errors are also plotted in Fig. 11(b) and Fig. 12(b). Figs. 11~12 all reveals that they have good position tracking and those results also show that the position tracking error in high frequency (3Hz) are larger than in low frequency (1Hz). Therefore, from Figs. 10~12, it demonstrates that the use of a TMS320F2812 DSP chip to construct a vector control and an adaptive fuzzy controller for PMSM drives in position loop is effectiveness, high performance and robustness.

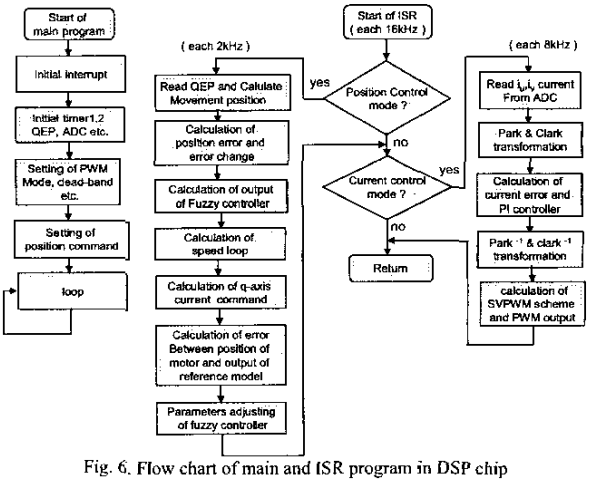

Fig. 6. Flow chart of main and ISR program in DSP chip

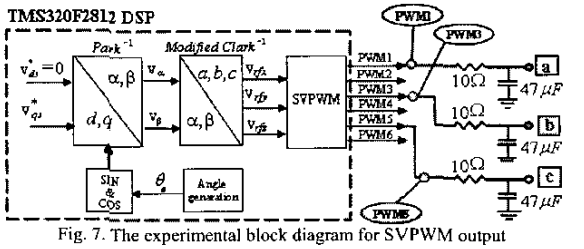

Fig. 7. The experimental block diagram for SVPWM output

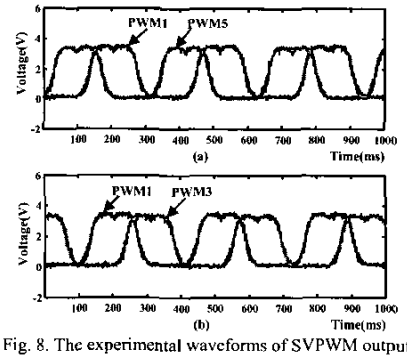

Fig. 8. The experimental waveforms of SVPWM output

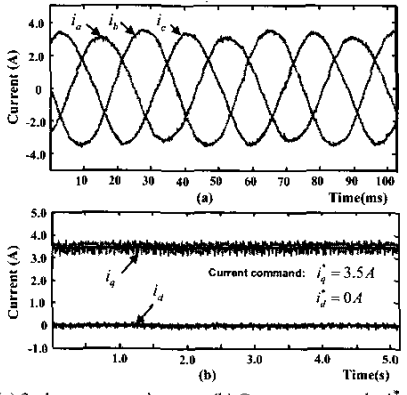

Fig. 9. (a) 3-phase measured current (b) Current commands i_d^*, i_q^* and measured currents i_d, i_q while adopting vector control

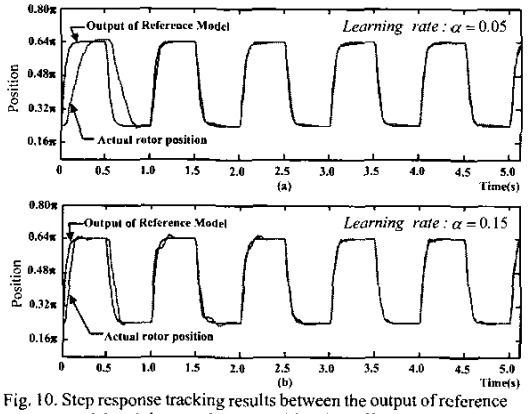

Fig. 10. Step response tracking results between the output of reference model and the actual rotor position for different learning rate (a) α=0.05 (b) α=0.15

IV. Conclusion

A high performance position controller for PMSM drives using a new generation TMS320F2812 DSP chip has been presented in this paper. In order to reach the high performance goals, those key techniques, such as the current vector controller, the SVPWM scheme and the adaptive fuzzy controller of the PMSM drives are all implemented in this DSP chip. Emulation result shows that even in the complicated operation of the proposed control algorithm, it only spends about 20μs computation time of DSP for executing an overall control loop. Experimental results also demonstrate that in step command response and frequency command response, the rotor position of PMSM can fast track the prescribed dynamic response well.

References

[1] B.K. Bose, *Power Electronics and Variable Frequency Drives – Technology and Application*, IEEE Press, 1997.

[2] B.K. Bose, "Expert System, Fuzzy Logic, and Neural Network Applications in Power Electronics and Motion Control," *Proc. IEEE*, vol. 82, no. 8, 1994, pp. 1303-1323.

[3] Y.S. Kung, C.M. Liaw and M.S. Ouyang, "Adaptive Speed Control for Induction Motor Drives Using Neural Networks," *IEEE Trans. on Indus. Electro.*, vol. 42, no.1, pp. 25-32, 1995.

[4] C.M. Liaw and Y.S. Kung, "Fuzzy Control with Reference Model-Following Response," *Fuzzy Theory Systems: Techniques and Applications*, vol.1, pp. 129-158, 1999.

[5] T.S. Radwan, M.A. Rahman, A.M. Osheiba and A.E. Lashine, "Dynamic Analysis of a High Performance Permanent Magnet Synchronous Motor Drive," *Electrical and Computer Engineering*, 1996, Canadian Conference on vol. 2, pp. 611-614.

[6] B. Zhang, Y. Li and Y. Zuo, "A DSP-based fully digital PMSM servo drive using on-line self-tuning PI controller" *Proc. PIEMC 2000*, vol.2, pp. 1012-1017.

[7] A.M. Trzynadlowski, M.P. Kazmierkowski, P.Z. Grabowski, M.M. Bech, "Three examples of DSP applications in advanced induction motor drives," *American Control Conference*, vol. 3, 1999, pp. 2139-2140.

[8] *TMS320F2810 and TMS320F2812 Digital Signal Processors*, Handbook of Texas Instruments, 2002.

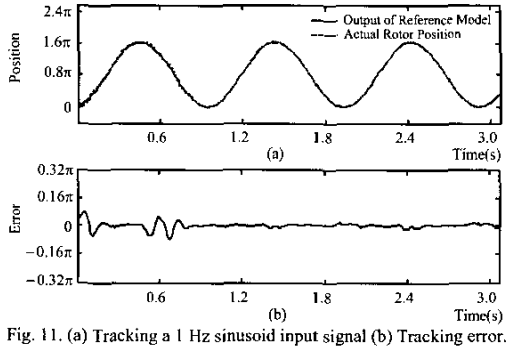

Fig. 11. (a) Tracking a 1 Hz sinusoid input signal (b) Tracking error.

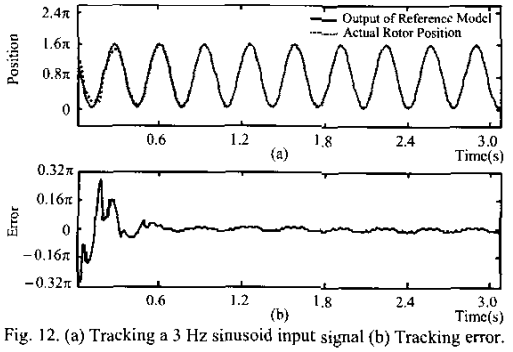

Fig. 12. (a) Tracking a 3 Hz sinusoid input signal (b) Tracking error.